

Blasting erosion arc machining of 20 vol.% SiC/Al metal matrix composites

Lin Gu¹ · Jipeng Chen¹ · Hui Xu¹ · Wansheng Zhao¹

Received: 16 November 2015 / Accepted: 23 March 2016 / Published online: 2 April 2016
© Springer-Verlag London 2016

Abstract Machining of metal matrix composite is a big challenge in industry for the high cutting tool cost and limited machining efficiency. In this study, blasting erosion arc machining (BEAM) was applied to improve the machining efficiency of SiC/Al composite. The performance of BEAM under negative and positive electrode machining conditions was investigated, and two sets of 3-factor, 2-level full factorial experiments were conducted to disclose the effects between the machining parameters. When the peak current was 500 A and the tool polarity was negative, the obtained MRR (material removal rate) was greater than 8270 mm³/min, and the TWR (tool wear ratio) was about 2 %. The competitive efficiency and economy of BEAM indicate the potential of electrical arcing in handling difficult-to-cut composite materials. The optimization of machining conditions can result in a high MRR which arrived to 10, 200 mm³/min, and the specific MRR was nearly three times of that of EDM. Furthermore, it was disclosed that the MRR in both negative and positive machining was sensitive to the peak current, pulse duration, and pulse interval while the TWR was appeared to be stable as the machining conditions varies within a certain range. The surface topography of the machined workpiece indicates that compared to the negative BEAM, positive BEAM creates a smoother surface under the same machining conditions. Furthermore, in order to study the

influence of SiC particles on the machining performance, a complementary experiment was conducted to compare the craters formed on 20 vol.% SiC/Al and pure aluminum. Based on the comparison results, it can be deduced that the discharging condition is possibly influenced by the SiC particles and result in smaller craters. Finally, a workpiece was machined to demonstrate the advantages of BEAM for the machining of SiC/Al composites.

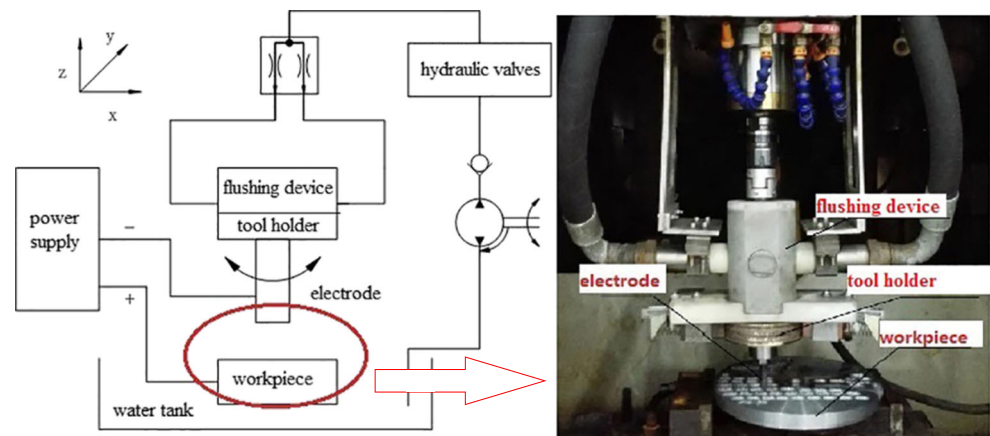
Keywords Blasting erosion arc machining · 20 vol.% SiC/Al · Efficiency · Polarity effects

1 Introduction

The metal matrix composites are playing more and more important roles in aerospace, energy, and biology industries because of their reinforced strength, modulus, wear and fatigue resistance [1]. As a typical metal matrix composite (MMC) material, SiC/Al components are usually machined by traditional cutting processes such as turning, drilling, and grinding. However, besides the strengthen effect, the reinforcing SiC particles also make it difficult to cut and lead to excessive tool wear. Karthikeyan et al. [2] studied the machining performance of SiC/Al composites with cemented carbide tool, and the reported MRR was about 5000 mm³/min (cutting speed 50 m/min, feed rate 0.1 mm/rev, cutting depth 1 mm, cutting time 1 min) for 20 vol.% SiC/Al composites. Ramanujam et al. [3] conducted turning experiments on 15 wt.% SiC (the corresponding volume fraction is about 12 %–15 %), and the maximum MRR was 17, 335 mm³/min (cutting speed 210 m/min, feed rate 0.25 mm/rev and cutting depth 0.6 mm), while the

✉ Lin Gu
lgu@sjtu.edu.cn

¹ State Key Laboratory of Mechanical System and Vibration, School of Mechanical Engineering, Shanghai Jiao Tong University, Shanghai 200240, China

Fig. 1 Experimental setup

machining parameters are not practicable because the CBN tool broke within 36 s. After considering the balance of the machining performance and tool life (up to 6.5 min), the optimized MRR was about $2700 \text{ mm}^3/\text{min}$ (cutting speed 90 m/min, feed rate 0.15 mm/rev, and cutting depth 0.2 mm).

Besides the cutting methods, SiC/Al composites can also be machined by non-traditional machining methods, such as electric discharge machining (EDM), wire electrical discharge machining (WEDM), and electrochemical machining (ECM). EDM is a typical method in processing electrical conductive difficult-to-cut materials, but the machining efficiency is limited. For instance, Mohan et al. [4] machined 20 vol.% SiC/Al composites with EDM and the achieved maximum MRR was $60 \text{ mm}^3/\text{min}$ (peak current 11 A, pulse duration 0.088 ms). Seo et al. [5] EDM drilled 20 vol.% SiC/Al and the MRR was about $140 \text{ mm}^3/\text{min}$ when the peak current was 100 A, and the pulse duration was 0.5 ms. In general, the MRR of EDM is much less than that of the cutting process, and the specific MRR is less than $6 \text{ mm}^3/(\text{A}\cdot\text{min})$.

Compared with the conventional EDM process, the arcing process has a higher energy density which leads to a much higher material removal rate. Up to

now, some researches have been reported about machining tough metals with electrical arcing, such as nickel-based alloys [6–10], steel [11], and titanium [12, 13]. However, reports about the machining performance of SiC/Al by electrical arcing are still unavailable. For the importance and specificity of metal matrix composites, it is necessary to research on the electrical arcing performance of this kind of difficult-to-cut material.

Zhao et al. [9] developed blasting erosion arc machining (BEAM) based on hydrodynamic arc breaking mechanism. By performing a strong multi-hole inner flushing, the arc plasma column in the discharge gap will be stretched, elongated, or even broken by the strong hydrodynamic force. When the arcing plasma column breaks, an extremely strong blasting occurs, and the coexisting shockwave blows off the molten material explosively from the molten pool on the workpiece. The BEAM can not only remove the difficult-to-cut materials in die-sinking mode but also in milling mode. In order to verify the feasibility of the BEAM, Xu et al. [14] machined nickel-based alloy with positive polarity BEAM utilizing a bundled electrode, besides, Chen et al. [15] studied the processing of titanium alloy with BEAM and machined a blade sample successfully.

Table 1 Full factorial experimental factors and levels

Factors	Levels	
	Low	High
Peak current, I_p (A)	100	500
Pulse duration, t_{on} (ms)	2	10
Pulse interval, t_{off} (ms)	1	9

Table 2 Comparison experimental parameters

	I_p (A)	t_{on} (ms)	t_{off} (ms)
Low energy	100	2	9
Moderate energy	300	6	5
High energy	500	10	1

Table 3 Results of negative electrode machining

Order	I_p (A)	t_{on} (ms)	t_{off} (ms)	MRR (mm^3/min)	TWR (%)
1	300	6	5	3827	2.58
2	500	2	1	5468	2.42
3	100	2	9	160	2.94
4	100	10	1	1950	3.10
5	100	10	9	800	2.61
6	100	2	1	1177	2.67
7	300	6	5	3800	2.62
8	500	10	9	7360	2.09
9	500	10	1	8276	2.02
10	500	2	9	3840	2.68

In this article, milling mode BEAM process was applied to machine SiC/Al composite workpiece. A 3-factor 2-level full factorial experiment was conducted to find out the relationship between the parameters and the machining performance. Besides, the influence of SiC particles on the crater size and depth was investigated by a comparison experiment between 20 vol.% SiC/Al and pure aluminum. Furthermore, the influence of machining polarity on machining performance was also studied. Finally, a sample workpiece was machined to demonstrate the advantage of BEAM on the machining of SiC/Al composite.

2 Experimental setup and conditions

2.1 Experimental setup

As shown in Fig. 1, a 5-axis BEAM machine was utilized to perform the experiments. The electrode is a cylindrical graphite electrode with 2 flushing holes, and the diameters of the electrode and the flushing holes are 10 and 2 mm, respectively. The electrode was fixed on a rotatable tool holder with 2 working

fluid inlets on both sides. The working fluid was water-based dielectric, and the workpiece was 20 vol.% SiC/Al composites.

2.2 Experimental conditions and procedure

Generally, in electrical arc machining process, the factors which affect the machining performance including the electrical parameters (such as peak current, pulse duration, pulse interval, and open voltage) and non-electrical parameters (such as flushing pressure, tool material, and rotating speed). Based on previous fractional factorial experiment, tool rotation speed and flushing pressure were found to have non-significant on MRR and TWR. Consequently, the electrode rotation speed was set to 1000 rpm, and the flushing pressure of the dielectric was set 2.0 MP_a in the experiment. During machining, the electrode fed in a layer milling mode and a series of 50-mm long and 3-mm deep slots were machined based on different experimental conditions. The open voltage of the power supplier was 90 V, and the gap voltage during machining was stabilized around 25 V.

The experiment consists of three sets.

- Set 1: negative electrode machining experiment (negative BEAM).
- Set 2: comparison experiment between 20 vol.% SiC/Al and pure aluminum.
- Set 3: positive electrode machining experiment (positive BEAM).

Experiment set 1 and set 3 were both designed as a 3-factor, 2-level full factorial experiment with 2 center points by Minitab software, and the only difference between set 1 and set 3 is the polarity of the electrode. The experimental conditions of set 1 are listed in Table 1.

Experiment set 2 was conducted after experiment set 1 to study the influence of SiC particles on the machining effect, and the experimental parameters consist of three

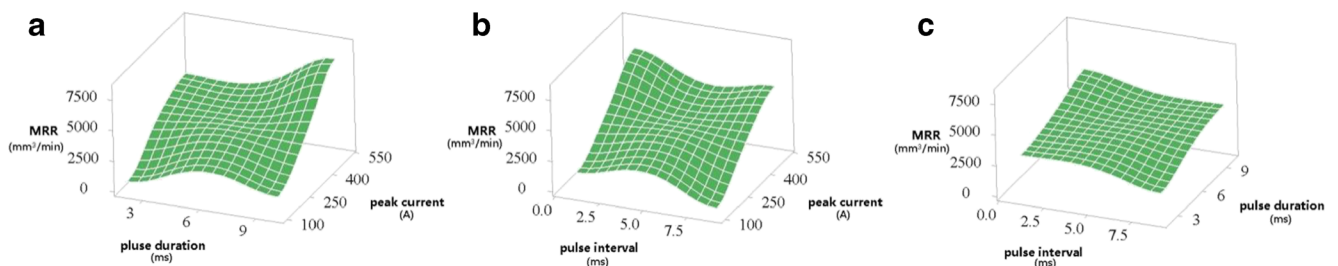


Fig. 2 Surface plots of MRR versus: **a** peak current, pulse duration, **b** peak current, pulse interval, and **c** pulse duration, pulse interval

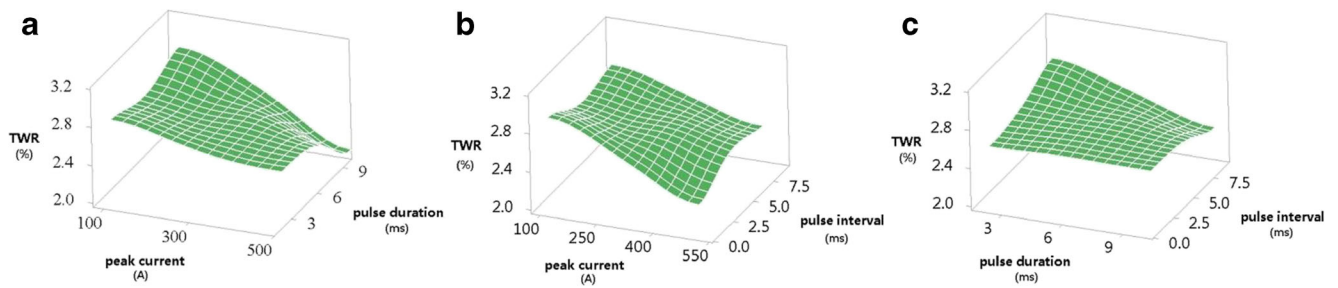


Fig. 3 Surface plots of TWR versus: **a** peak current, pulse duration, **b** peak current, pulse interval, and **c** pulse duration, pulse interval

energy levels, as listed in Table 2. Besides, a group of single discharge generated craters under the low energy condition ($I_p=100$ A, $t_{on}=2$ ms, and $t_{off}=9$ ms) was observed on the condition of stationary dielectric. For each material, 5 craters were generated and observed.

After the experiments, the workpiece surface was observed by a scanning electron microscope (SEM, type: JSM7800F), and the section view was taken by metallographic microscope (type: ZEISS Axio Imager A1m), single discharge craters were observed by confocal microscopy (type: ZEISS LSM 700). Besides, the compositions of the machined surfaces were analyzed by energy dispersive spectrometer (EDS, type: Thermo NORAN 7). And the residual stresses were measured by X-ray diffraction (XRD, type: Proto-LXRD) at different depths.

3 Results of negative electrode machining (negative BEAM) and discussion

Results of negative electrode machining are shown in Table 3.

3.1 Material removal rate (MRR)

Figure 2 shows surface plots of MRR versus peak current, pulse duration and pulse interval.

The full factorial experiment result discloses that besides the three main factors, the interaction between peak current and pulse duration also has a main effect on MRR. The influence of other cross inter-factor

interactions on material removal rate is negligible. In general, MRR increases with the peak current and pulse duration, but declines with the pulse interval. This can be explained from the view point of discharge energy. The inputted energy in each discharging/arc period is determined by the gap voltage, peak current, and pulse duration. For the gap voltage is generally stable during arcing, the energy will increase when the peak current and pulse duration raise but decrease when the pulse duration is longer. The highest MRR was $8276 \text{ mm}^3/\text{min}$ when the peak current was 500 A and the pulse duration was 10 ms, which means the specific MRR was $16.4 \text{ mm}^3/(\text{A}\cdot\text{min})$, much higher than that of EDM (MRR $140 \text{ mm}^3/\text{min}$ when peak current was 100 A) as reported [5]. It is obvious that even for the difficult-to-cut material such as SiC/Al composites, BEAM could still achieve a rather high MRR. According to the analyzing results of the factors significance, a fitting formula is given

$$\text{MRR} = 423.37 + 8.43 I_p + 11.44 t_{on} - 147.27 t_{off} + 0.77 I_p \times t_{on} \quad (1)$$

3.2 Tool wear ratio (TWR)

Figure 3 shows the surface plots of TWR versus peak current, pulse duration and pulse interval.

Experimental results show that the TWR varies in a limited range when the machining parameters change (about 1 %). The maximum TWR was 3.10 % ($I_p=100$ A, $t_{on}=10$ ms, $t_{off}=1$ ms), and the minimum

Table 4 Optimized value and experimental test

	$\times 1$ (A)	$\times 2$ (ms)	$\times 3$ (ms)	MRR (mm^3/min)	Specific MRR ($\text{mm}^3/(\text{min} \cdot \text{A})$)	TWR (%)
Optimized value	600	10	1	10,069	16.78	1.82
Experimental result	600	10	1	10,200	17.0	1.80
Error (%)	–	–	–	1.28	0.19	1.11

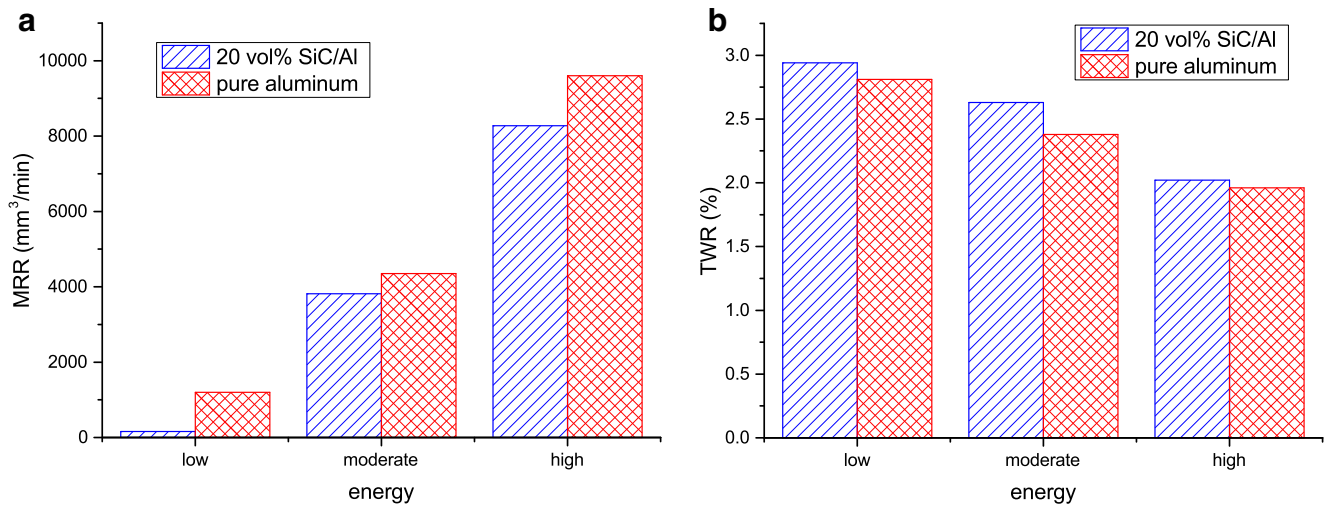


Fig. 4 Comparison of machining performance between 20 vol.% SiC/Al and pure aluminum: **a** MRR and **b** TWR

TWR was 2.02 % ($I_p=500$ A, $t_{on}=10$ ms, $t_{off}=1$ ms). Further analysis disclosed that only the peak current and the interaction of peak current and pulse duration are significant for TWR. TWR is apt to decrease when the peak current and pulse duration increase. This tendency is just opposite to that of the MRR and could be explained from the view point of discharge plasma conditions; when the peak current is limited (e.g., 100 A), the discharge plasma density is prone to be affected by the gasified semi-conductive SiC molecules, and this would led to a poor discharge condition and decrease the energy efficiency; when the peak current is higher (e.g., 500 A), the discharge plasma density would be higher, which means it is difficult to be impacted by the SiC particles, and the tool consumption would decrease as the result of the increasing energy efficiency. After removing the non-

significant factors, a fitting formula of TWR is given as following

$$TWR = 2.829 - 0.000297I_p + 0.020 t_{on} - 0.00017 I_p \times t_{on} \quad (2)$$

3.3 Optimization of MRR

In order to magnify the MRR, the parameters were optimized with MATABL optimization toolbox according to the fitting formulas (1) and (2). The machining parameters were set according to the range of power supplier: $I_p \in (100,600)$ (600 A is the maximum peak current of the power source), $t_{on} \in [1, 10]$ and $t_{off} \in [1, 10]$. In the constraints, TWR was set in the range of 1 to 3 %, and the specific MRR was set between 16.0 to 18.0 (mm³/min.A). The optimization and experimental

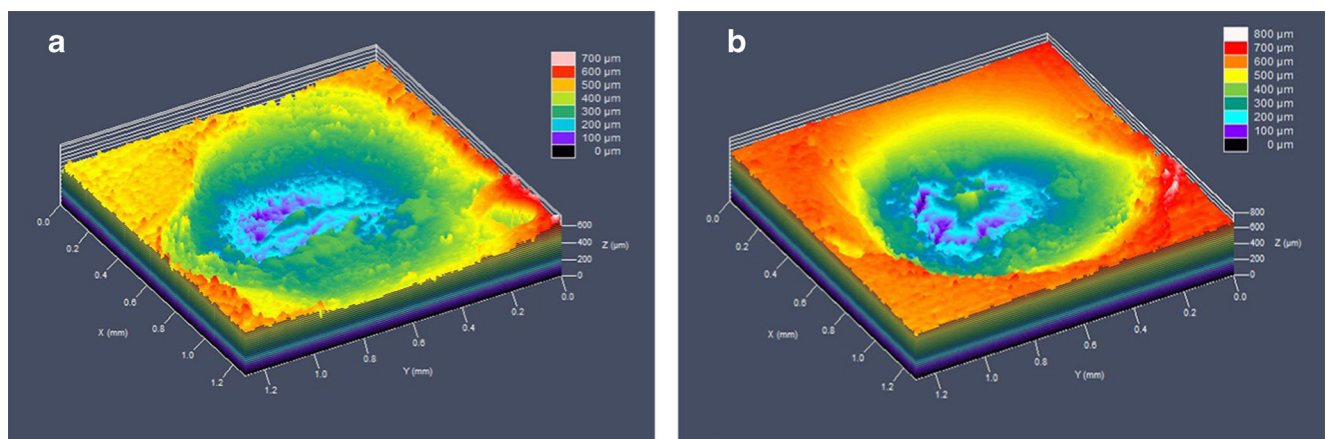


Fig. 5 Single discharge crater comparison: **a** 20 vol.% SiC/Al and **b** pure aluminum

Table 5 Single discharge craters of 20 vol.% SiC/Al and pure aluminum under low energy condition

	20 vol.% SiC/Al			Pure aluminum		
	Maximum diameter (mm)	Maximum depth (mm)	Volume (mm ³)	Maximum diameter (mm)	Maximum depth (mm)	Volume (mm ³)
Crater 1	0.9479	0.310	1.1670	1.115	0.360	1.1150
Crater 2	0.9828	0.228	0.7404	1.0354	0.350	1.0830
Crater 3	1.1604	0.393	0.5818	1.0178	0.310	0.9618
Crater 4	1.0304	0.320	0.9964	1.1129	0.330	0.9021
Crater 5	1.0954	0.278	0.7046	1.1654	0.340	0.9669
Mean value	1.0434	0.3058	0.8380	1.0893	0.3380	1.0058
Variance	0.00587	0.00293	0.04526	0.00301	0.00029	0.00642

results are listed in Table 4. According to the optimization results, when the peak current was 600 A, pulse duration was 10 ms and pulse interval was 1 ms, MRR could reach about 10,200 mm³/min, the specific MRR could be up to 17.0 mm³/(min.A), and TWR is about 1.80 %.

Errors of MRR between the optimized value and the experimental value are within less than 2 %, which indicates the MRR's optimization process is acceptable.

4 Results of comparison experiment and discussion

Comparison experiment set 2 was designed to study the influence of SiC particles on the BEAM of 20 vol.% SiC/Al composites, and the results are shown in Fig. 4.

Compared to the MRR of aluminum, the MRR of SiC/Al decreases obviously, and the TWR also increases slightly even under the same machining conditions. It is obvious that the SiC particles have dominate influence on the machining performance, especially on the MRR, since

Table 6 Results of positive electrode machining

Order	I _p (A)	t _{on} (ms)	t _{off} (ms)	MRR (mm ³ /min)	TWR (%)
1	300	6	5	2417	3.53
2	500	2	1	3840	3.23
3	100	2	9	160	4.31
4	100	10	1	1920	3.53
5	100	10	9	640	3.92
6	100	2	1	640	3.20
7	300	6	5	2410	3.54
8	500	10	9	3840	3.69
9	500	10	1	4800	2.78
10	500	2	9	2560	3.27

the SiC particles have a different electrical conductivity and heat conduction with the pure aluminum. Firstly, the SiC particles make the electrical conductivity of the SiC/Al worse; secondly, the sublimated SiC (over 2700 °C) in the discharging channel will also reduce the ionization ratio of the plasma and led to lower energy density. With the mentioned reasons, MRR declines, and the corresponding TWR increases during BEAM machining of SiC/Al. A group of single discharge craters was compared and shown in Fig. 5, and the characteristics of all the craters were listed in Table 5.

From Table 5, it can be found that the discharge craters of 20 vol.% SiC/Al are smaller and shallower than that of pure aluminum; hence, the average volume of 20 vol.% SiC/Al craters is 16.7 % smaller than the other. Besides, the variance of depth and volume of 20 vol.% SiC/Al craters are almost 7–10 times of that of the pure aluminum, which indicates the discharge plasma is weakened by the SiC during machining.

5 Results of positive electrode machining (positive BEAM) and discussion

Although BEAM is applied to remove bulk material with a high material removal rate, an acceptable surface is also necessary for the further post processing. In BEAM process, the polarity of electrode has a significant influence on the machining performance, especially the MRR and surface quality. So it is necessary to investigate the polarity effect on BEAM of SiC/Al composite. Positive electrode machining was complemented as set 3, and the results are shown in Table 6.

5.1 Material removal rate (MRR)

Since the MRR is mainly determined by the discharge energy, the MRR of positive machining increases with

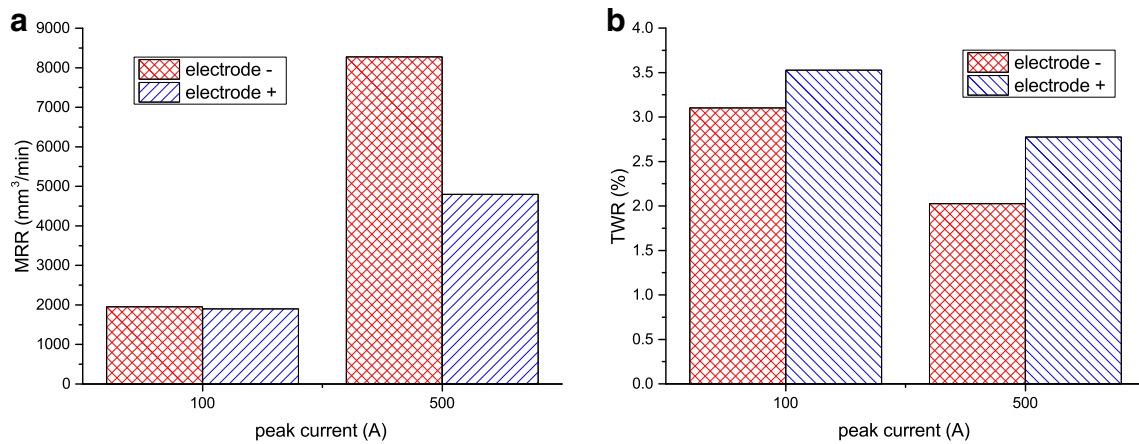


Fig. 6 Comparison between different polarities, $t_{on} = 10$ ms, $t_{off} = 1$ ms: **a** MRR and **b** TWR

the peak current and pulse duration while declines with the elongation of pulse interval. These characters are similar to that of the negative polarity machining. When the peak current was 500 A, pulse duration was 10 ms and the pulse interval was 1 ms, the MRR of a positive BEAM was about 4800 mm³/min, still much higher than that of the EDM processing. The regressed formula of the MRR of a positive electrode machining can be expressed as

$$MRR = -15 + 7.3I_p + 125t_{on} - 125t_{off} \quad (3)$$

5.2 Tool wear ratio (TWR)

The maximum TWR in the experiments was about 4.31 % ($I_p = 100$ A, $t_{on} = 2$ ms and $t_{off} = 9$ ms), and the minimum TWR was about 2.78 % ($I_p = 500$ A, $t_{on} = 10$ ms and $t_{off} = 1$ ms). Although the TWR of positive BEAM is slightly higher than that of negative BEAM, the values of TWR under different parameters are still within a narrow range, similar to that of the negative BEAM. DOE (design of experiment) analyzing results by Minitab disclosed that TWR is significantly affected by the peak current, pulse duration, and the

interaction effects of current, pulse duration, and pulse interval. The regressed formula for TWR is

$$TWR = 3.5 - 0.2487 I_p - 0.0113 t_{on} + 0.3063 t_{off} - 0.0687 I_p \times t_{off} + 0.1987 I_p \times t_{on} \times t_{off} \quad (4)$$

5.3 Comparison with negative BEAM

A typical comparison of MRR and TWR of negative and positive polarity machining is shown in Fig. 6. In general, when machining SiC/Al with positive BEAM, the efficiency is lower than that of negative BEAM, and the tool wear is relatively higher. A possible explanation is that during discharging, more energy is distributed to the anode than that to the cathode [16].

Although the decline of peak current in negative BEAM can improve the surface roughness, the machined surfaces are still very rough. For contrast, under the same parameters in positive BEAM, the discharged craters become smaller and homogeneously. As shown in Fig. 7, the surfaces machined by positive BEAM are much smoother and brighter than that of negative BEAM even under the same machining conditions. As mentioned above, since the energy distributed on the anode is higher, the discharge craters are

Fig. 7 Comparison of machined surfaces, $t_{on} = 10$ ms, $t_{off} = 1$ ms: **a** negative BEAM, $I_p = 100$ A, **b** negative BEAM, $I_p = 500$ A, **c** positive BEAM, $I_p = 100$ A, and **d** positive BEAM, $I_p = 500$ A

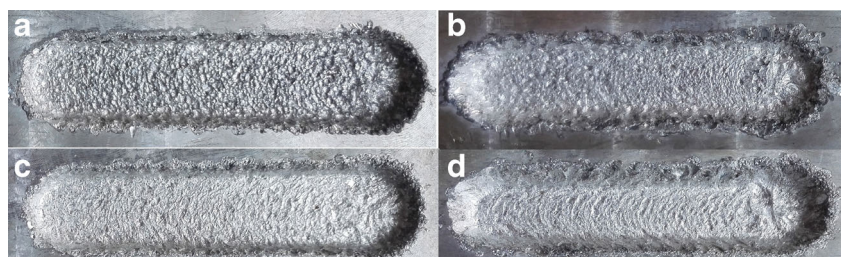
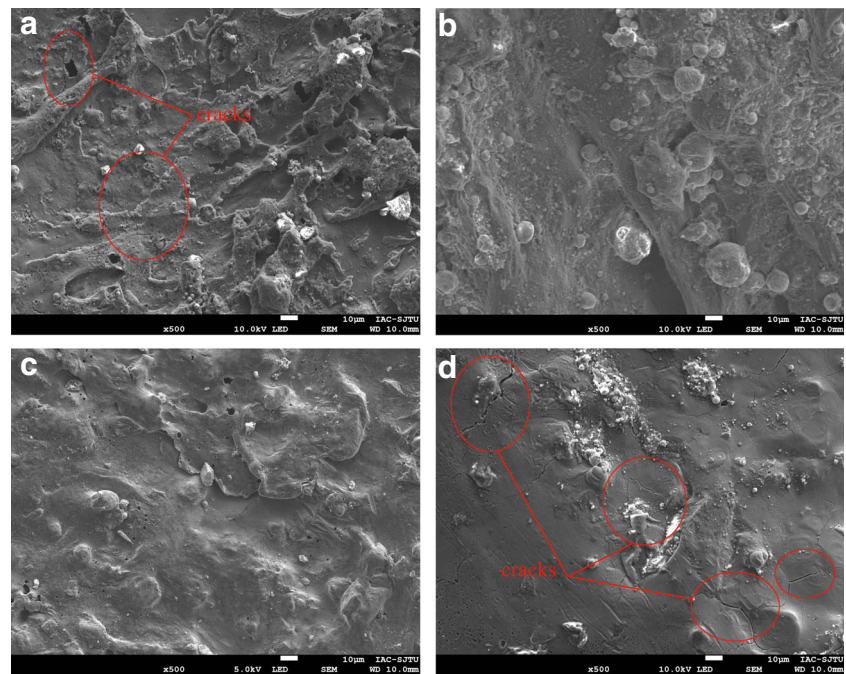


Fig. 8 Machined surfaces observed by SEM, $t_{on} = 10$ ms, $t_{off} = 1$ ms: **a** negative BEAM, $I_p = 100$ A, **b** negative BEAM, $I_p = 500$ A, **c** positive BEAM, $I_p = 100$ A, and **d** positive BEAM, $I_p = 500$ A



consequently larger, which means the surface is rougher. Besides, the oxygen ions move to the anode under effect of the electric field, which is apt to result in the oxidation and ablation of material at the anode.

The comparison above indicates that a large peak current with negative electrode is suitable for bulk mass material removal, while the positive electrode processing can be used to refine the surface before further processing.

5.4 Comparison of machined surface

The machined surface by different polarity BEAM with 500 A peak current and 10-ms pulse duration was observed by scanning electron microscope (SEM). As shown in Fig. 8, the negative BEAM machined workpiece has a rough and mushy surface that formed by collision debris. A positive BEAM machined surface, however, is much smoother. It is noted that some micro-cracks

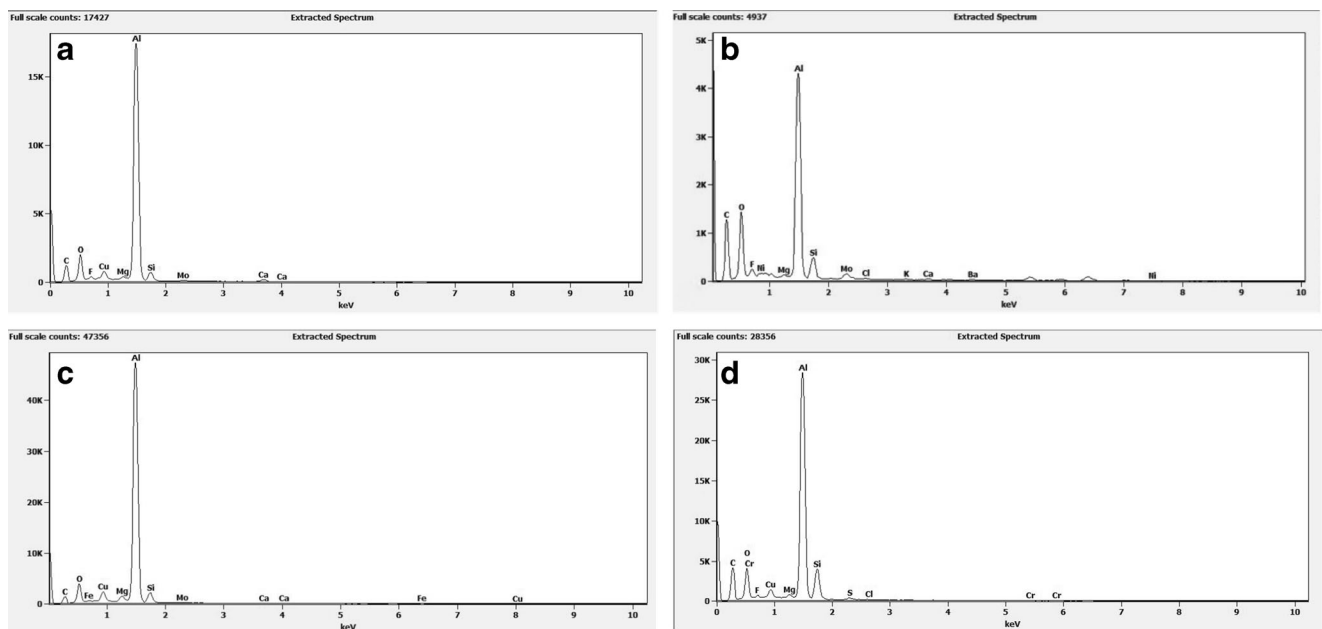
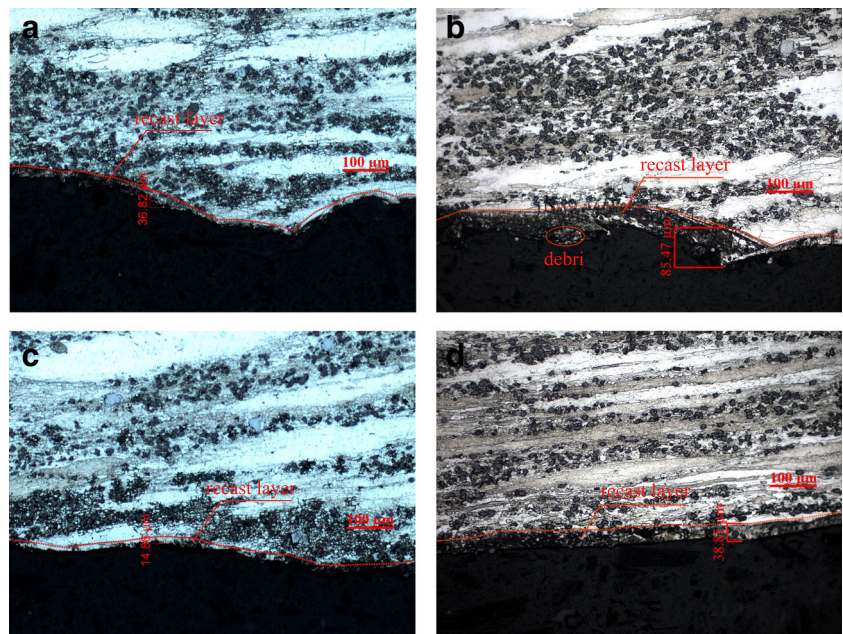


Fig. 9 EDS results, $t_{on} = 10$ ms, $t_{off} = 1$ ms: **a** negative BEAM, $I_p = 100$ A, **b** negative BEAM, $I_p = 500$ A, **c** positive BEAM, $I_p = 100$ A, and **d** positive BEAM, $I_p = 500$ A

Fig. 10 Metallographic photo of the machined workpiece, $t_{on} = 10$ ms, $t_{off} = 1$ ms: **a** negative BEAM, $I_p = 100$ A, **b** negative BEAM, $I_p = 500$ A, **c** positive BEAM, $I_p = 100$ A, and **d** positive BEAM, $I_p = 500$ A



can be found under both negative and positive electrode machined surfaces, which is similar to the EDM process [5].

Energy-dispersive spectrometer (EDS, worked in face scan mode) tests for element compositions in Fig. 8 are presented in Fig. 9. Under the same machining parameters, the negative polarity machined surface contains more scale of oxygen and carbon that is why the surface appeared to be grey and the positive polarity machined surfaces appeared to be silvery.

The cross-sectional morphology was observed by metalloscope and shown in Fig. 10. It can be disclosed that for the negative BEAM, the recast layer is much thicker and varies in a large scope. Besides, some debris are adhering on the machined surface. For the positive BEAM, the debris can be removed efficiently, and the thickness of the recast layer tends to be thin and uniform.

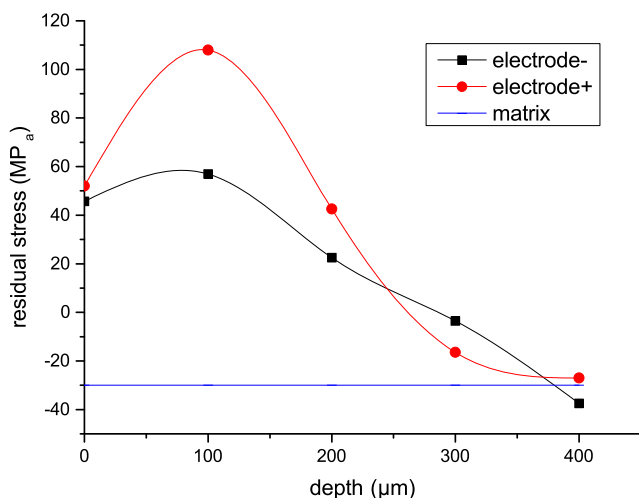


Fig. 11 Residual stress tests by XRD, $I_p = 500$ A, $t_{on} = 10$ ms, $t_{off} = 1$ ms

Figure 11 shows the X-ray diffraction (XRD) results of residual stress of the workpiece machined with different machining polarities. The residual stress was measured every 0.1 mm in depth by electrochemically eroding the surface material layer by layer. It is clear that the residual stress of both negative and positive machined surfaces is close to that of the material matrix (about -30 MPa) after the depth is deeper than 0.4 mm. Consequently, it is recommended that when machining 20 vol.% SiC/Al composites with BEAM, the allowance of following process should be greater than 0.4 mm.

6 Sample workpiece machining

A SiC/Al composite workpiece was machined with the optimized parameters, and Fig. 12a shows the workpiece after rough machined by BEAM. The dimension of the workpiece was 430 mm × 270 mm × 22 mm. When machining with conventional cutting processes, the rough machining time was more than 12 h. While with BEAM, the time expended for rough machining was about 2 h, about one fifth of that of the referred conventional cutting processes (rough cutting). Even considering the finish machining, over two thirds of the total machining time can be saved. Figure 12b shows the finished workpiece after the milling process.

7 Conclusions

1. The BEAM process is competent for the machining of SiC/Al composites with a high efficiency. For machining

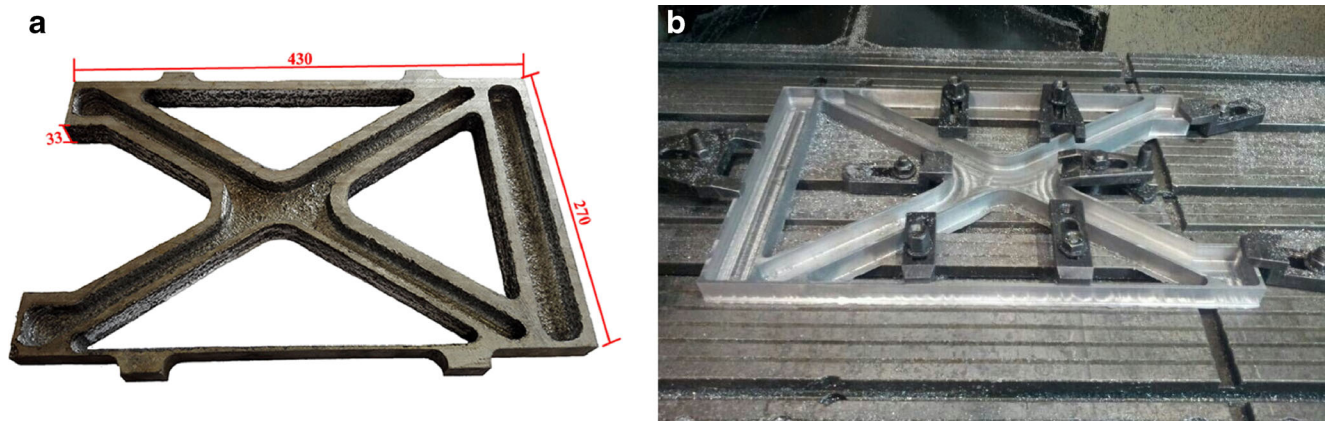


Fig. 12 SiC/Al workpiece: **a** rough machining by BEAM and **b** finish machining by cutting processes

20 vol.% SiC/Al composites with negative BEAM, the optimized MRR can be up to 10,200 mm³/min when peak current is 600 A, pulse duration was 10 ms, and pulse interval was 1 ms.

2. The SiC particles in the matrix influence the discharging conditions and result in a smaller crater as well as lower MRR and higher TWR.
3. The MRR is sensitive to the peak current, pulse duration, and pulse interval in both negative and positive BEAM, while the TWR is relative stable with a limited variation range.
4. A positive BEAM produces a smoother surface than that of negative BEAM. Consequently, a large peak current with negative electrode is suitable for bulk mass material removal, and the positive electrode machining is recommended to achieve a better surface for further processing.

Acknowledgments This work is supported by the Natural Science Foundation of China (grant no. 51235007 and no. 51575351), the State Key Laboratory of mechanical system and vibration Focus Fund, Shanghai Jiao Tong University (GrantNo.MSV201305), the Joint Foundation of SJTU, and CASC (grant no. USCAST2015-19). Besides, the authors also acknowledge the tests developed at Instrumental Analysis Center of SJTU.

References

1. Song M (2009) Effects of volume fraction of SiC particles on mechanical properties of SiC/Al composites. *Trans Nonferrous Metals Soc China* 19:1400–1404. doi:10.1016/S1003-6326(09)60040-6
2. Karthikeyan R, Ganesan G, Nagarajan RS, Pai BC (2001) A critical study on machining of Al/SiC composites. *Materials Manuf Process* 16(1):47–60. doi:10.1081/AMP-100103696
3. Radhakrishnan R, Muthukrishnan N, Raju R (2011) Optimization of cutting parameters for turning Al-SiC(10p) MMC using ANOVA and grey relational analysis. *Int J Precis Eng Manuf* 12(4):651–656. doi:10.1007/s12541-011-0084-x
4. Mohana B, Rajadurai A, Satyanarayana KG (2004) Electric discharge machining of Al-SiC metal matrix composites using rotary tube electrode. *J Mater Process Technol* 153–154:978–985. doi:10.1016/j.jmatprotec.2004.04.347
5. Seo YW, Kim D, Ramulu M (2006) Electrical discharge machining of functionally graded 15–35Vol% SiC/Al composites. *Mater Manuf Process* 21:479–487. doi:10.1080/10426910500471482
6. Trimmer AL, Hayashi S, Lamphere M (2010) Advancement in high speed electro-erosion processes for machining tough metals. *Proceedings of the 16th International Symposium on Electromachining*. Shanghai
7. Ye J, Wu G, Wang F, Wu Q, Xu L, Luo G (2011) The orthogonal test and reach on the optimum parameters of the pulse power in NC high performance electrical-discharge milling. *Electromachining Mould* 2011(6):16–20
8. Wang F, Liu Y, Shen Y et al (2013) Machining performance of Inconel 718 using high current density electrical discharge milling. *Mater Manuf Process* 28:1147–1152. doi:10.1080/10426914.2013.822985
9. Zhao W, Gu L, Xu H et al (2013) A novel high efficiency electrical erosion process—blasting erosion arc machining. *Procedia CIRP* 6: 621–625. doi:10.1016/j.procir.2013.03.057
10. Yuan R, Wei B, Luo Y et al (2010) High-speed electroerosion milling of superalloys. *ISEM-16*, Shanghai: 207–210
11. Wang F, Liu Y, Tang Z, Ji R, Zhang Y, Shen Y (2014) Ultra-high speed combined machining of electrical discharge machining and arc machining. *Proc Inst Mech Eng B J Eng Manuf* 228(5):663–672. doi:10.1177/0954405413506194
12. Wang F, Liu Y, Zhang Y (2014) Compound machining of titanium alloy by super high speed EDM milling and arc machining. *J Mater Process Technol* 214:531–538. doi:10.1016/j.jmatprotec.2013.10.015
13. Chengbo G, Shichun D, Dongbo W, Yunlong S, Xiang W (2015) Research on efficient electrical discharge milling of TC4 titanium alloy. *Acta Armamentarii* 36(11):2149–2156. doi:10.3969/j.issn.1000-1093.2015.11.020
14. Xu H, Gu L, Chen J et al (2015) Machining characteristics of nickel-based alloy with positive polarity blasting erosion arc machining. *Int J Adv Manuf Technol* 79(5–8):937–947. doi:10.1007/s00170-015-6891-y
15. Chen J, Gu L, Xu H, et al (2015) Study on blasting erosion arc machining of Ti–6Al–4V alloy[J]. *Int J Adv Manuf Technol*:1–11. doi:10.1007/s00170-015-8126-7
16. Xia H, Hashimoto H, Kunieda M et al (1996) Measurement of energy distribution in continuous EDM process. *J JSPE* 62(8): 1141–1145. doi:10.2493/jjspe.62.1141